#41

Phase Transitions, 1979, Vol. 1, pp. 1–22
0141–1594/79/0101–0001 $04.50/0

Printed in Great Britain

Polyhedral Tilting: A Common Type of Pure Displacive Phase Transition and Its Relationship to Analcite at High Pressure

ROBERT M. HAZEN and LARRY W. FINGER

Geophysical Laboratory, Carnegie Institution of Washington, Washington, D.C. 20008, U.S.A.

(*Received July 15, 1978; in final form October 17, 1978*)

Polyhedral tilt transformations are a subgroup of pure displacive solid-solid phase transitions that occur in many ionic compounds and have all the following characteristics: (1) the transitions occur in compounds with structures composed of corner-linked, rigid polyhedral elements; (2) transitions are between a higher-symmetry or less-distorted form (stable at higher temperature or lower pressure) and a lower-symmetry or more-distorted form (stable at lower temperature or higher pressure); (3) transitions are nonquenchable, and single crystals are preserved through the transition; (4) twinning is common in the low-symmetry form, with the twin law governed by a symmetry operator lost in the high-to-low transition; (5) the value of dP/dT is always positive and is similar to the ratio of large-site thermal expansivity to compressibility.

Analcite, $(NaAl)_xSi_{3-x}O_6 \cdot H_2O$ with $0.9 < x < 1.0$, is a zeolite mineral that undergoes several polyhedral tilt transitions. Under room conditions analcites are pseudo-cubic; seven dimensionally distinct varieties are cubic, tetragonal $c < a$ and $c > a$, orthorhombic, monoclinic with b parallel to pseudo-cubic [110] or [100], and triclinic. Several phase transitions have been detected from unit-cell measurements at high pressure on single crystals. At 4 kbar, orthorhombic and tetragonal analcites become monoclinic (C centered) with b parallel to pseudo-cubic [110]. No volume change is observed at this transition. At 8 kbar a volume discontinuity greater than 1 percent is observed. At 12 kbar dimensionally-monoclinic analcite becomes triclinic with no apparent volume change. At about 18 kbar a second volume discontinuity of 0.25 percent is observed, indicating a fourth transition. All these transitions conform to the criteria of polyhedral tilt transitions.

INTRODUCTION

Solid-solid phase transformations are important to all physical sciences and are a major focus in mineralogy and petrology. Attempts to understand these transformations and their mechanisms have been aided by several

classification schemes based on structural, thermodynamic, kinetic, or other observational grounds (Heuer and Nord, 1976). Buerger (1951, 1972) recognized two major structural groups of phase transitions: reconstructive, in which some primary bonds are broken, and displacive or reversible, in which secondary bonds may be broken but primary bonds are unaffected. Megaw (1973) further subdivided reversible transitions into four categories, including "pure displacive," in which "topology is completely unchanged." Pure displacive transitions may involve small cation displacements (as in $BaTiO_3$) or tilting of polyhedral elements of the structure (as in α-β quartz). Buerger (1972) described the latter type of displacive transition in terms of high-temperature "thermal agitation," and all his examples are high-temperature (high-symmetry) to low-temperature (low-symmetry) forms. Recent studies have demonstrated that polyhedral tilt transitions are also common at high pressure (Hazen, 1977a,b). These high-pressure transitions are closely related—in geometry, twinning, and symmetry—to the high-temperature polyhedral tilt transitions, and a more general treatment of this common transition mechanism is therefore warranted. The principal objectives of this study are to define and characterize polyhedral tilt transitions as a subgroup of pure displacive transitions and to apply this analysis to the description of high-pressure analcite phase transitions.

POLYHEDRAL TILT TRANSITIONS

Several characteristics are common to all polyhedral tilt transitions and may be used to distinguish them from other types of transformations.

1) Polyhedral tilt transitions occur in ionic† compounds with corner-linked, rigid cation-anion groups, such as tetrahedral Al-Si groups in framework silicates, or octahedral groups in perovskites. The framework of rigid polyhedra may form large cation sites (i.e. Na^+ in feldspar or Ba^{2+} in gillespite) or cavities or channels (as in quartz or zeolites). Polyhedral tilt transitions occur when polyhedral elements of the rigid framework tilt owing to the changing size of the large cation site or cavity with changing pressure or temperature.

2) The transition is between a high-symmetry or less-distorted form (stable at higher temperature or lower pressure) and a low-symmetry or more-distorted form (stable at lower temperature or higher pressure).

3) The transition is rapid, reversible, and nonquenchable; single crystals are preserved through the phase change.

† Ionic compounds include oxides and halides, in which atoms may be treated as cations and anions in the sense used by Pauling (1960).

4) Twinning is commonly introduced in transforming from the higher-symmetry to the lower-symmetry form. The twin law is governed by a symmetry operator of the high-symmetry phase that is lost in the transition.

5) The transition is geometrically related to the size of the large site or cavities; therefore, $(dP/dT) = (\partial P/\partial T)_{v \text{ of large site}}$ = the ratio of thermal expansivity to compressibility (α/β) for the large site.

Of the five characteristics common to all polyhedral tilt transitions, (3) and (4) are generally true of pure displacive transitions. In some cation-displacement transitions characteristic (1), as in $BaTiO_3$, or characteristic (2), as in calcite I $\rightleftarrows$ II, may also be observed. We know of no cation-displacement transition, however, in which all five characteristics occur. In the $BaTiO_3$ transition dP/dT is negative (Clarke and Benguigui, 1977), and in calcite I $\rightleftarrows$ II the structure is not composed of corner-linked polyhedra (Merrill and Bassett, 1974a). Many examples of polyhedral tilt transitions are known, and several are listed in Table I.

Geometry of transformation

All polyhedral tilt transitions result from the greater compressibilities and thermal expansivities of weakly bonded large-cation polyhedra compared to the surrounding corner-linked, rigid polyhedra. As a high-symmetry or less-distorted structure (the "high" form) is cooled or compressed toward a polyhedral tilt transition, the large site or cavity becomes smaller at a greater rate than the rigid, linked polyhedra. A transition to a low form occurs at a critical minimum size of the large site. In general, a slight structural rearrangement by tilting of corner-linked, small-cation polyhedra causes a decrease in large-site volume with little or no change in the size of rigid polyhedra. Tilting of corner-linked polyhedra will have an effect on lattice parameters that is dependent on structure type and degree of tilt (Megaw, 1973). Each structure type, therefore, must be analyzed separately in relating structural changes to unit-cell dimensions.

Polyhedral tilt transitions may be described geometrically, because the size of the large site or cavity governs which form is observed. The high form has the greater large-site volume, and this volume can be reduced to the critical size by a reduction in temperature, an increase in pressure, or substitution of a smaller cation into the large site.† The nature of the transition in

† At high temperatures the mechanism of polyhedral tilt transitions may not be due to large-site size alone. In the $\alpha \rightleftarrows \beta$ quartz transition at room pressure and $T \approx 573°C$, for example, the high-symmetry form may result from rapid transitions between twin-related small domains of α-quartz due to thermal agitation rather than exist as a true "nontitled" structure. The effect of this thermal averaging, however, is the same as an increase in size of the large site.

TABLE I

Polyhedral tilt transitions

Mineral	Formula	Transition cond. T(°C)	Transition cond. P(kbar)	dP/dT (bar/°C)	Space group: High form	Space group: Low form	Ref.
Quartz	SiO_2	573	0	+40	$P6_222$ / $P6_422$	$P3_221$ / $P3_121$	Cohen *et al.* (1974)
Carnegieite	$NaAlSiO_4$	707	0	+125			Cohen and Klement (1976)
Perovskite-type	$NaNbO_3$						
$a^\circ a^\circ a^\circ \leftrightarrow a^\circ a^\circ c^+$		640	0	—	*Pm3m*	*F4/mmb*	Megaw (1974)
$a^\circ a^\circ c^+ \leftrightarrow a^- b^\circ c^+$		575	0	—	*F4/mmb*	*Ccmm*	
$a^- b^\circ c^+ \leftrightarrow a^- b^+ c^+$		520	0	—	*Ccmm*	*Pnmm*	
Clinoenstatite	$MgSiO_3$	980	0		*C2/c*	$P2_1/c$	Smyth (1974)
Gillespite	$BaFeSi_4O_{10}$	23	12	—	*P4/ncc*	$P2_12_12$	Hazen (1977a)
Sanidine	$KAlSi_3O_8$	23	24	+15	*C2/m*	$C\bar{1}$	Hazen (1976)
High Albite/Monalbite	$NaAlSi_3O_8$	~1100	0				
Cordierite(disordered)	$Al_3Mg_2(Si_5Al)O_{18}$	>1400	0	—	*P6/mcc*	*Cccm*	Langer and Schreyer (1969)
Deerite	$Fe^{2+}_{12}Fe^{3+}_6Si_{12}O_{40}(OH)_{10}$	~600			*Pna2₁ or Pnma*	$P2_1/a$	Agrell (pers. comm.)
Analcite	$NaAlSi_2O_6 \cdot H_2O$						
I ↔ II		23	7	+57			This Study
II ↔ III		23	19	—			

pressure-temperature-composition space, therefore, will be similar for all polyhedral tilt transitions, as illustrated in Figure 1. Note, for example, that dP/dT will always be positive, because a lowering of pressure has the same effect on large-site volume as a raising of temperature. Furthermore, the magnitude of dP/dT, a macroscopic property, will be similar to the polyhedral $\bar{\alpha}/\bar{\beta}$, where $\bar{\alpha}$ and $\bar{\beta}$ are the mean linear polyhedral thermal expansivity and compressibility, respectively, of the large site (Hazen and Prewitt, 1977). Polyhedral tilt transitions, therefore, are examples of the similarity of structural variations due to changes in temperature, pressure, and composition (Hazen, 1977b).

Many mineral structure types should not display polyhedral tilt transitions, as the requirement of corner-linked arrays of rigid polyhedral elements is not satisfied. Orthosilicates and most layer silicates, oxides of divalent and trivalent cations, and carbonates and nitrates, as well as nonionic minerals, will not undergo polyhedral tilting.

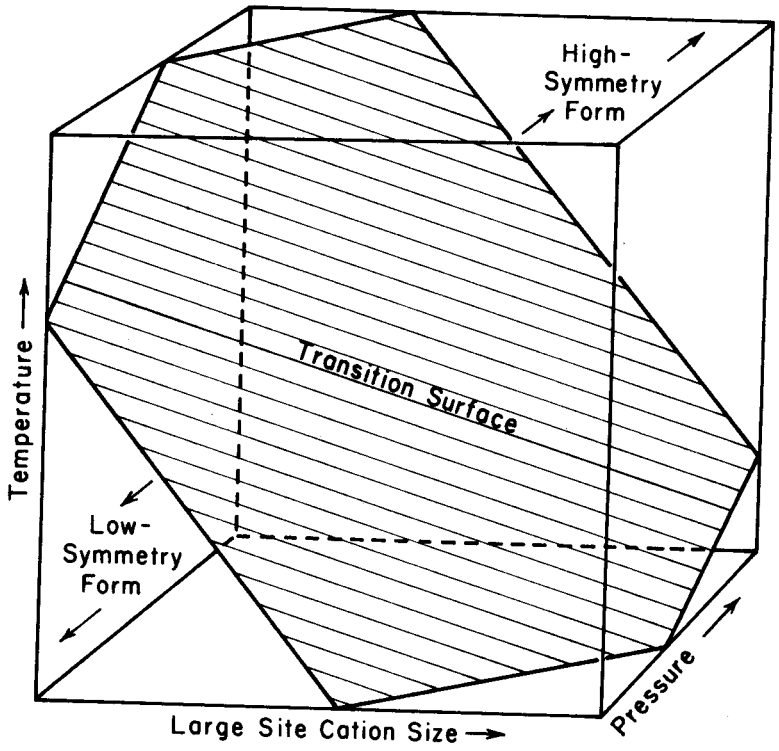

FIGURE 1 Idealized transition surface for a polyhedral tilt transition in pressure-temperature-composition space. In all polyhedral tilt transitions $\partial P/\partial T > 0$, $\partial r/\partial T < 0$, and $\partial r/\partial P > 0$, where r is the average radius of the large-site cation.

Symmetry

The tilted form is the lower-symmetry or more-distorted form in polyhedral tilt transitions. Strens (1967) demonstrated that in reversible transitions involving a change of symmetry, the high-temperature form is also the form with greater degeneracy of normal vibration modes and consequently has the higher symmetry. It follows that the low-pressure form will also have the higher symmetry because dP/dT is positive. Strens also emphasized the important point that reversible transitions in which there is a discontinuity of volume need not be accompanied by a change in symmetry.

A symmetry change in polyhedral tilt transitions generally involves the removal of a symmetry operator of the high-symmetry form. In second-order structural transitions this relationship is rigorously true (Boccara, 1968), because the lower-symmetry form must have a unit cell and space group that are subgroups of the higher-symmetry form. Supergroup-subgroup relationships are seen, for example, in the $\alpha \rightleftarrows \beta$ quartz, monalbite $\rightleftarrows$ high albite, and several perovskite transitions. In first-order polyhedral tilt transitions (e.g. those with nonzero ΔV) this space-group relationship is not always observed, as in the gillespite I $\rightleftarrows$ II phase transition (Hazen, 1977a).

Preservation of single crystals

An important characteristic of polyhedral tilt transitions, at least from an experimentalist's point of view, is that crystals are preserved through the transition. The slight rearrangements of structural elements, even if several weak metal-oxygen bonds are broken,† are not sufficient to destroy the external morphology of the sample. It is possible, therefore, to measure the variation of directional properties in crystals through the transition.

Polyhedral tilt transitions are nonquenchable. A high-pressure or high-temperature form will invert to the room-condition structure immediately upon lowering of temperature or pressure. In some first-order polyhedral tilt transitions (e.g. gillespite I $\rightleftarrows$ II) a slight hysteresis may be present, but this effect is small. These transitions, therefore, must be studied in situ at high temperature or high pressure.

Twinning

Twinning is a common, if not ubiquitous, consequence of a symmetry reduction in polyhedral tilt transitions. The topologies of both low- and high-symmetry forms are closely related, and there exists at least a two-fold ambiguity in the orientation of the low-symmetry form because of the

† Polyhedral tilt transitions may involve a change in primary coordination of the large site. In cubic perovskites, for example, there are twelve oxygen atoms around the A site, whereas orthorhombic perovskites may have nine-coordinated A sites.

removal of a symmetry element. Twinning is introduced, therefore, in transitions from high- to low-symmetry forms, with the twin law determined by a symmetry element of the high-symmetry phase lost during transformation.

Polyhedral tilt twinning may reveal useful information if the symmetry relations of the transition twins are known. The presence of this type of twinning in a crystal may provide evidence that the crystal at some time existed in the high-symmetry form and was subsequently cooled below the transition. In quartz, for example, Dauphiné twins indicate cooling from the untwinned β phase; and twinning in cordierite, deerite, nepheline, and other collapsed structures may also provide information on thermal history. The absence of the specific type of twinning associated with polyhedral tilting, on the other hand, may imply a low temperature of crystallization within the low-symmetry phase region. In addition, twinning induced in high-pressure, collapsed forms such as gillespite II may aid in the interpretation of the structure of the high-pressure form (Hazen, 1977a), as identification of the twin law should indicate the nature of the large-site distortion. Note, however, that compounds that have polyhedral tilt transitions at high pressure will not show the transition-associated twinning under room conditions.

Polyhedral tilt twins complicate the determination of some structures (deerite, for example) under room conditions. One solution is to determine the high-symmetry structure at high temperature first and then proceed to determine the related structure of the twinned modification under room conditions. It should also be noted that synthetic crystals grown below the transition temperature are less likely to be twinned and may provide better material for single-crystal studies or commercial use.

Identification of polyhedral tilt transitions

Polyhedral tilt transitions are best recognized and described in terms of complete structural refinements of the high and low forms. For crystals at high temperature or high pressure, or crystals that are twinned, such data are frequently not obtainable. Identification of tilt transformations in these materials must rest provisionally on conformity with the five essential criteria outlined above. The zeolite mineral analcite (or analcime) is an example of a substance that undergoes several pure displacive transitions at high pressure but for which high-pressure structural data are not available. The remainder of this study is devoted to the description and analysis of these transitions as probable examples of polyhedral tilt transitions.

Analcite at room pressure

Polyhedral tilt transitions are sensitive to the composition and structure of the compound undergoing transformation. It is essential, therefore, to

document the composition and structure of analcite under room conditions before describing the high-pressure forms. Nineteen analcites were selected from specimens of the Department of Mineralogy and Petrology, Cambridge University, and from the U.S. National Museum of Natural History, Washington, D.C., as listed in Table II. Electron microprobe analyses of these specimens are reported in Table III, along with partial optical data. Analcites with less than 0.1 wt percent K_2O lie close to the line for ideal analcites of composition $(NaAl)_xSi_{3-x}O_6 \cdot H_2O$ with $0.9 < x \leq 1.0$. Analcites with greater than 0.1 wt percent K_2O may be significantly depleted in total alkalis and therefore plot below the ideal line for Na + Al $\rightleftarrows$ Si, as illustrated in Figure 2. None of the analcites studied has a value of K/(Na + K) greater than 0.02; Na-K solid solution, therefore, appears to be less extensive than Na + Al $\rightleftarrows$ Si in natural analcites.† Other possible compositional variations of analcite have been discussed by Deer *et al.* (1963) but do not appear to be significant in terms of the compositions reported in Table III.

Ideal disordered analcite is cubic (space group $Ia3d$) with $a \approx 13.7$ A and $Z = 16$; however, ordering of aluminum and silicon among tetrahedral sites of the framework will reduce the symmetry. Most analcites are slightly birefringent, suggesting small but significant deviations from the ideal cubic form; and previous X-ray diffraction studies (Coombs, 1955; ASTM card 19-1180; Mazzi and Galli, 1978) have revealed tetragonal, rhombohedral, and monoclinic, as well as essentially cubic analcites. From single-crystal structural refinements Mazzi and Galli (1978) have demonstrated that at least some of these deviations from cubic symmetry are due to Al/Si ordering in the tetrahedral framework.

Unit-cell dimensions of sixteen analcite single crystals (Table IV) were measured on an automated four-circle diffractometer using the procedure described by Hamilton (1974) and modified by H. King and L. W. Finger (in preparation) whereby errors in the crystal centering and diffractometer alignment are removed by measuring reflections in eight different positions. Of the sixteen analcites studied, only three are dimensionally cubic within 2.5 estimated standard deviations.‡ Four of the analcites are dimensionally

† The "high-K analcites" of Larsen and Buie (1938), which reportedly had greater than 20 atom percent K in alkali sites, actually have finely disseminated Or-rich feldspar (Wilkinson, 1968) and a brownish iron-bearing phase (hematite?), which lead to erroneous bulk chemical analyses. Electron microprobe analysis of this material (Table III, No. 4) reveals only 2 atom percent K in alkali sites.

‡ Dimensional symmetry is based on unit-cell dimensions only. Complete structural refinements were not made, and actual analcite symmetry may be lower than the reported dimensional symmetry. Dimensional symmetry is the highest possible crystal system within 2.5 estimated standard deviations of the observed unit-cell dimensions. Crystals known to be cubic rarely deviate by more than 2.5 *esd*'s from true cubic dimensions when treated as triclinic using the stated procedures.

TABLE II

Analcite specimen localities and museum specimen numbers

Number	Locality	Museum number[a]	Host rock and comments
1	Cyclopian Islands, Sicily	CU 777	On basalt
2	Kilpatrick Hills, Ireland	CU 557	
3	Phoenix Mine, Lake Superior, Michigan	CU 776	
4	Highwood Mtns., Montana	Harvard FBH169	Phenocrysts in basalt
5	Wasson's Bluff, Nova Scotia	USNM 96299	Cavities in basalt
6	Bergen Hill, New Jersey	USNM 8363	Cavities in basalt
7	Lambert Quarry, Benton County, Oregon	USNM 16508	
8	City Water Tunnel, Baltimore, Maryland	USNM 136528	Massive veins in basalt
9	De-Mix Quarry, Mt. St. Hillaire, Quebec	USNM 132507	
10	Cyclopian Islands, Sicily	CU-Wilshire Coll.	On basalt
11	RR Quarry, Ardglen, New South Wales	USNM 96528	
12	Table Mtn., Golden, Colorado	USNM 84842	Cavities in basalt
13	County Antrim, Ireland	CU 743	
14	Faroe Islands	CU-Wilshire Coll.	
15	Paterson, New Jersey	USNM 133312	Cavities in basalt
16	Frombach, Seiser Alps, Italy	USNM 115751	Reddish crystals in basalt cavity
17	Monti Catini, Val Cecina, Italy	USNM B17262	Variety "picranalcime"
18	Rinocovo, Monchique, Algarve, Portugal	USNM B17294	
19	Taseq near Narssaq, SW Greenland	USNM 133763	Massive white analcite

[a] CU = Cambridge University; USNM = United States National Museum

TABLE III

Analcite electron microprobe analyses and optical data

Specimen Number	1	2	3	4	5	6	7	8	9
Number of points	6	6	6	10	6	6	6	8	6
SiO_2	54.6	55.5	56.8	57.4	57.4	55.7	56.7	57.2	54.2
Al_2O_3	23.9	22.7	21.7	24.4	21.9	22.3	21.7	21.4	22.7
MgO	0.00	0.00	0.00	0.17	0.01	0.01	0.00	0.01	0.03
CaO	0.82	0.00	0.04	0.51	0.04	0.04	0.08	0.02	0.02
Na_2O	12.7	13.8	13.1	10.4	13.1	13.4	13.1	12.9	14.2
K_2O	0.11	0.08	0.03	0.49	0.00	0.00	0.00	0.00	0.04
Total[a]	92.1	92.1	91.7	93.4	92.5	91.5	91.6	91.5	91.6
$\bar{n}(\pm 0.001)$[b]	1.489	1.486	1.485	1.494	1.485	1.486	1.485	1.485	1.485
δ[c]	<0.001	0.001	0.001	<0.001	0.000–0.003	≤0.001	≤0.002	0.001	0.001
Number of ions on the basis of 6 oxygen plus H_2O.									
Si	1.99	2.03	2.07	2.03	2.07	2.04	2.06	2.08	2.01
Al	1.03	0.97	0.93	1.02	0.93	0.97	0.96	0.92	0.99
Na	0.89	0.97	0.95	0.77	0.92	0.95	0.95	0.91	1.02
Ca	0.03	0.00	0.00	0.02	0.00	0.00	0.00	0.00	0.00
K	0.01	0.00	0.00	0.02	0.00	0.00	0.00	0.00	0.00

[a] Total based on 6 oxygens. H_2O excluded from total. $TiO_2 < 0.02$ wt.% in all analyses. FeO < 0.1% except No. 4 (see footnote on page 8).

[b] $\bar{n}$ is the average index of refraction measured in white light.

[c] δ is the birefringence.

TABLE III—*continued*

Specimen Number	10	11	12	13	14	15	16	17	18	19
Number of points	6	7	15	6	6	7	7	7	6	6
SiO_2	54.8	55.3	56.7	55.5	54.6	55.1	54.7	56.9	54.8	55.3
Al_2O_3	23.8	22.2	22.4	22.6	22.2	22.5	22.4	21.2	22.2	23.5
MgO	0.00	0.00	0.00	0.02	0.00	0.00	0.00	0.00	0.00	0.00
CaO	0.84	0.03	0.04	0.00	0.04	0.02	0.03	0.04	0.04	0.01
Na_2O	13.1	12.6	13.7	13.5	13.1	13.4	13.1	12.7	12.7	13.8
K_2O	0.03	0.06	0.01	0.01	0.06	0.00	0.08	0.07	0.00	0.02
Total[a]	92.6	90.2	92.8	91.5	90.0	91.2	90.3	90.9	89.7	92.6
$\bar{n}(\pm 0.001)$[b]	1.488	1.486	1.484	1.486	1.487	1.487	1.485	1.484	1.485	1.490
δ[c]	≤ 0.001	0.002	0.002	< 0.001	0.002	0.001	0.0015	0.001	≤ 0.001	0.002
Number of ions on the basis of 6 oxygen plus H_2O.										
Si	1.99	2.05	2.05	2.03	2.03	2.02	2.03	2.09	2.04	2.00
Al	1.02	0.97	0.95	0.97	0.97	0.98	0.98	0.92	0.97	1.00
Na	0.92	0.90	0.96	0.96	0.94	0.95	0.94	0.90	0.92	0.97
Ca	0.03	0.00	0.00	0.00	0.00	0.00	0.00	0.00	0.00	0.00
K	0.00	0.00	0.00	0.00	0.00	0.00	0.00	0.00	0.00	0.00

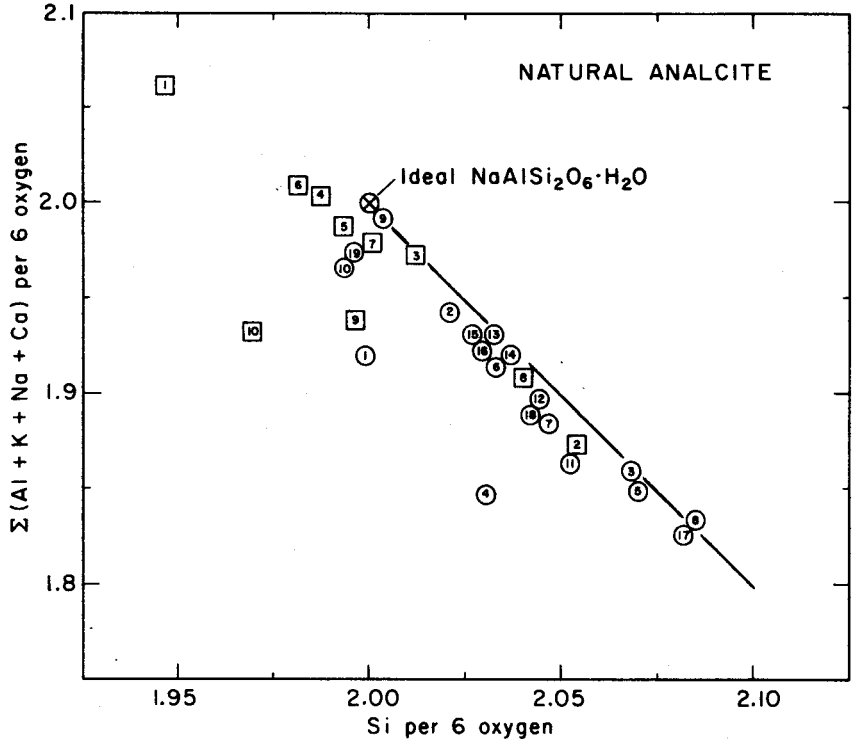

FIGURE 2 Compositional variation of natural analcites. The major observed variation is given by the formula $(NaAl)_xSi_{3-x}O_6 \cdot H_2O$, as indicated by the solid line. Squares mark specimens as numbered by Deer *et al.* (1963, Table 44); circles mark specimens of this study (see Tables II–V).

tetragonal (two with $c > a$ and two with $c < a$) and two are orthorhombic; the remaining seven specimens have nonorthogonal unit cells. The true symmetry of these nonorthogonal, body-centered, pseudo-cubic unit cells is not obvious from the values reported in Table IV. The dimensional symmetry is best determined by examining the *S*-matrix of the reduced unit cell (Buerger, 1957). This analysis indicates that four analcites (Nos. 7, 8, 10, and 13) may be described by a pseudo-cubic *I*-centered monoclinic unit cell, with the 2-fold axis parallel to a pseudo-cubic [100]. Two analcites (Nos. 9 and 14) are *C*-centered monoclinic with the 2-fold axis parallel to a pseudo-cubic [110]. The true monoclinic unit cell is approximately $a = 13.7, b = 19.3, c = 11.9$ Å, and $\beta = 125°$. The remaining analcite is triclinic within 2.5 standard deviations, although it is close to *C*-centered monoclinic in dimensions.

Useful parameters in describing the deviation of the pseudo-cubic unit cell from true cubic dimensions are Δa, defined as the difference between the

TABLE IV

Analcite unit-cell parameters, deviations from cubic dimensions, and suggested crystal systems at 1 bar

Sample Number[a]	a(A)	b(A)	c(A)	α(°)	β(°)	γ(°)	V(A^3)	Δa(A)[b]	$\Delta\alpha$(°)[c]	System[d]
1	13.708(2)[e]	13.709(2)	13.732(2)	89.98(2)	89.98(2)	89.97(2)	2580.5(6)	0.024(4)	0.03(2)	T+
2	13.693(7)	13.710(12)	13.743(9)	89.99(6)	89.99(5)	89.95(6)	2580.1(3.2)	0.050(16)	0.05(6)	T+
3	13.697(3)	13.696(3)	13.714(6)	90.00(3)	90.00(3)	89.98(2)	2572.6(1.5)	0.018(9)	0.02(2)	C
4	13.707(2)	13.712(1)	13.714(2)	89.98(1)	90.025(11)	89.995(9)	2577.8(6)	0.007(4)	0.025(11)	C
5(δ = 0.000)	13.706(6)	13.704(4)	13.713(4)	89.98(3)	89.96(4)	90.00(3)	2576.6(1.6)	0.009(8)	0.04(4)	C
5(δ = 0.003)	13.668(1)	13.718(1)	13.721(1)	90.001(7)	89.966(7)	89.913(8)	2576.4(4)	0.053(2)	0.02(2)	T−
6	13.693(2)	13.713(3)	13.715(4)	89.99(2)	89.98(2)	90.00(1)	2575.3(1.0)	0.022(6)	0.02(2)	T−
7	13.6994(11)	13.7069(8)	13.7075(6)	89.991(4)	89.998(5)	89.963(8)	2573.9(3)	0.0081(17)	0.037(8)	M
8	13.679(2)	13.709(1)	13.712(2)	89.956(9)	90.000(11)	89.981(11)	2571.4(5)	0.023(4)	0.044(9)	M
9	13.7136(10)	13.7291(12)	13.7353(8)	89.979(6)	89.980(6)	89.982(7)	2586.0(3)	0.022(2)	0.021(6)	M′
10	13.7140(5)	13.7256(6)	13.7351(6)	89.970(4)	90.006(3)	89.992(4)	2585.4(2)	0.0211(11)	0.030(4)	M
11	13.7014(15)	13.7224(12)	13.7340(12)	90.005(7)	89.988(8)	89.999(10)	2582.2(4)	0.033(3)	0.012(8)	O
12	13.703(2)	13.714(2)	13.724(3)	90.05(2)	90.01(1)	90.04(2)	2579.0(9)	0.021(5)	0.05(2)	O
13	13.7013(12)	13.7113(9)	13.7277(12)	89.994(6)	90.010(9)	89.979(7)	2578.9(4)	0.0264(24)	0.021(7)	M
14	13.6967(10)	13.7184(11)	13.7286(10)	89.967(6)	89.965(6)	90.088(6)	2579.6(3)	0.0319(20)	0.088(6)	M′
15	13.6824(5)	13.7044(6)	13.7063(5)	90.158(3)	89.569(3)	89.545(3)	2569.9(2)	0.0239(10)	0.455(3)	Tr

[a] See Tables II and III for sample descriptions.

[b] Δa is the difference between the longest and shortest pseudo-cubic a axis. Parenthesized figures represent the sum of *esd*'s for these two lengths.

[c] $\Delta\alpha$ is the maximum deviation from 90° for the three pseudo-cubic cell angles. Parenthesized figures represent the *esd*'s associated with these angles.

[d] The highest possible crystal system within 2.5 times *esd*'s of observed unit-cell dimensions. C = cubic; T+ = tetragonal with $c > a$; T− = tetragonal $c < a$; O = orthorhombic; M = monoclinic with 2-fold axis parallel to pseudo-cubic [100]; M′ = monoclinic with 2-fold axis parallel to pseudo-cubic [110]; Tr = triclinic.

[e] Parenthesized figures represent *esd*'s of least units cited.

maximum and minimum pseudo-cubic edge lengths, and $\Delta\alpha$, defined as the maximum angular deviation from 90° of the three pseudo-cubic unit-cell angles. These values are recorded in Table IV for room-pressure analcites; the average deviations are 0.02 Å and 0.06°, respectively, for Δa and $\Delta\alpha$ at room pressure. There is no definite correlation between analcite birefringence (Table III) and deviation parameters Δa and $\Delta\alpha$. Birefringence, however, is generally lower for cubic analcites than for monoclinic and triclinic analcites. In specimen No. 5 from Wasson's Bluff, Nova Scotia, a range of birefringence is observed. A grain with no observable birefringence (Table IV, No. 5a) has cubic dimensions, whereas a grain with $\delta = 0.003$ (Table IV, No. 5b) is tetragonal, $c < a$. Birefringence in analcites may therefore be due to a combination of noncubic dimensions and internal strain.

High-pressure phase transitions of analcite

Yoder and Weir (1960) demonstrated that analcite undergoes a rapid and reversible phase transition at approximately 8 kbar based on high-pressure X-ray powder diffraction, and they suggested that the transition is to a phase with analcite-type structure slightly distorted from ideal cubic symmetry. Rosenhauer and Mao (1975) confirmed this observation and determined dP/dT as 0.057 kbar/°C using differential thermal analysis. Details of the unit-cell variation with pressure were not determined by previous workers. One objective of this study was to determine the nature of analcite compression to pressures above the observed 8 kbar volume discontinuity.

EXPERIMENTAL

Single crystals of a tetragonal analcite from Cyclopian Islands (Tables II and III, No. 1), approximately 100 × 100 × 40 μm with the short dimension parallel to [010], and an orthorhombic analcite from Golden, Colorado (Tables II and III, No. 12), approximately 150 × 140 × 45 μm with the short dimension parallel to [101], were selected for study at high pressure. Crystals were mounted in miniature diamond cells (Merrill and Bassett, 1974b) using 4 : 1 methanol-ethanol as the hydrostatic pressure medium. Ruby fragments less than 10 μm maximum dimension were included in the mount for pressure calibration by the R_1 fluorescence line shift (Piermarini *et al.*, 1975). Pressure cells were attached to modified goniometer heads (Hazen and Finger, 1977), and unit-cell dimensions were measured using reflection centering on a four-circle diffractometer as described above. Unit-cell data in Table V provide information on analcite compressibility, which is isotropic within the error of measurement. Linear compressibility is 8.4×10^{-4} kbar^{-1} (bulk modulus

0.40 ± 0.01 Mbar), in close agreement with values reported by Yoder and Weir (1960).

TRANSFORMATIONS

Analcite unit-cell dimensions at high pressure are listed in Table V and illustrated in Figures 3 and 4. These data indicate a complex transformation behavior of analcite between 0 and 25 kbar, with two significant volume discontinuities at approximately 8 and 19 kbar and two possible symmetry changes at approximately 4 and 12 kbar. Below 4 kbar the two analcites studied at high pressure have orthogonal unit cells; Cyclopian analcite is tetragonal (assumed to be $I4_1/acd$ after Mazzi and Galli, 1978) and Golden, Colorado, analcite is orthorhombic (*Ibca*). At pressures above 4 kbar but below the first volume discontinuity, both analcites deviate from orthogonality. Analysis of the reduced cells indicates that analcites in this pressure range are *C*-centered monoclinic with cell dimensions approximately $a = 13.6$, $b = 19.3$, $c = 11.8$ Å, and $\beta = 125.1°$. The two-fold b axis of the monoclinic cell is parallel to pseudo-cubic [110] so that this first high-pressure phase is geometrically similar to specimens 9, 14, and 15 at room pressure (Table IV). There is no observable volume change at this orthogonal-to-monoclinic transition, which may therefore be second order.

At the first volume discontinuity a significant increase in distortion from the ideal cubic unit cell is observed. Deviation parameters of $\Delta a > 0.06$ Å and $\Delta\alpha > 0.8°$ are significantly greater than values below the transition. No change in dimensional symmetry is observed, however, and the *C*-centered monoclinic cell at 10 kbar is approximately $a = 13.6$, $b = 19.2$, $c = 11.6$ Å, and $\beta = 124.7°$. The volume change for Cyclopian analcite at 6.5 kbar is 1.1 percent, and the volume change for Golden analcite at 8.5 kbar is 1.6 percent. This second analcite phase transition is apparently the one observed by Yoder and Weir (1960) and Rosenhauer and Mao (1975). Above the first volume discontinuity several reflections were observed to split into strong and weak components. This splitting was small at pressures near the transition, and peak-centering was more difficult for some of these reflections. Errors in unit-cell parameters consequently are larger for these pressures. The exact nature of the high-pressure twinning was not determined owing to the difficulty in resolving the weak components of split reflections.

At pressures above 12 kbar both analcites deviate from monoclinic dimensions, indicating a third *possible* transition from *C*-centered monoclinic to triclinic. The reduced primitive triclinic cell has axes along three of the four ⟨111⟩ axes of the pseudo-cubic cell, with approximate dimensions at 18 kbar of $a = 11.6$, $b = 11.8$, $c = 11.8$ Å, $\alpha = 109.4$, $\beta = 109.2$, $\gamma = 109.2°$. There is no observed volume discontinuity at 12 kbar, and it is not possible to

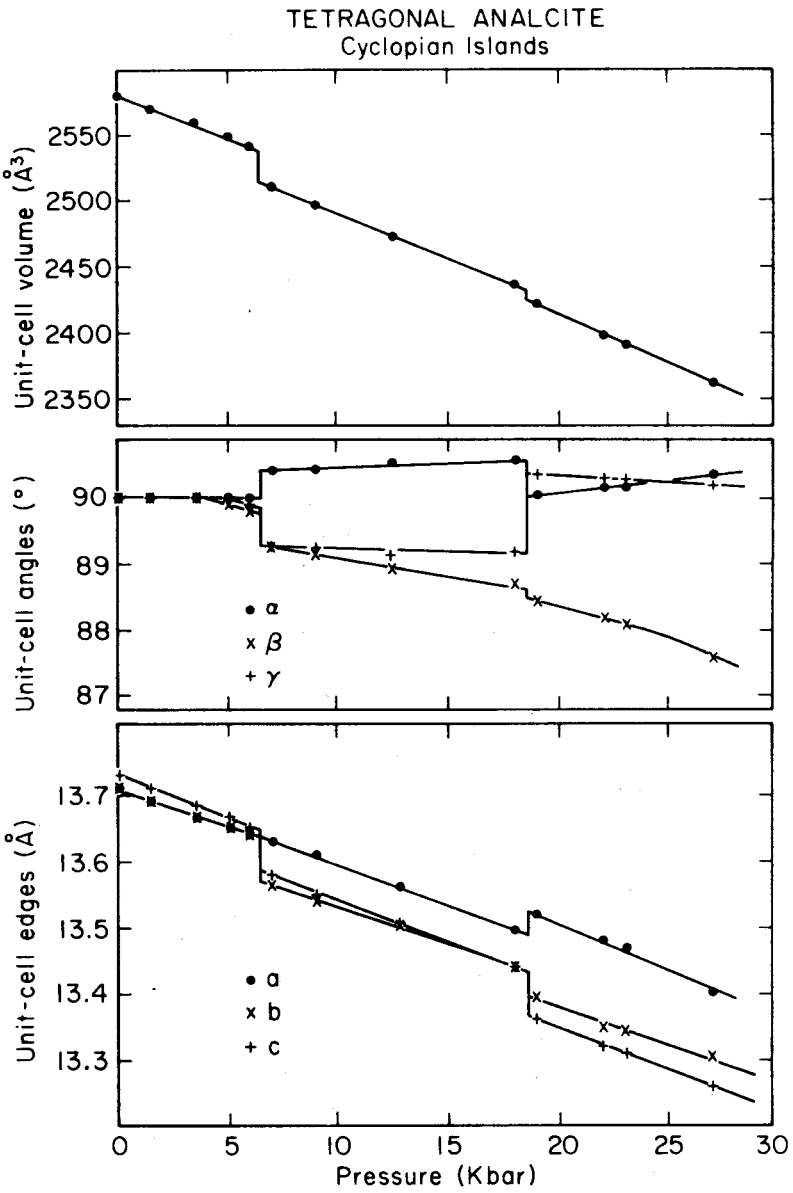

FIGURE 3 Unit-cell parameters vs. pressure for tetragonal analcite from the Cyclopian Islands. Two volume discontinuities, at 6.5 and 18.5 kbar, and two changes in dimensional symmetry, at about 4 kbar (tetragonal to monoclinic) and at 12 kbar (monoclinic to triclinic) suggest there are four polyhedral tilt transitions in analcite below 25 kbar. Compare with Figure 4.

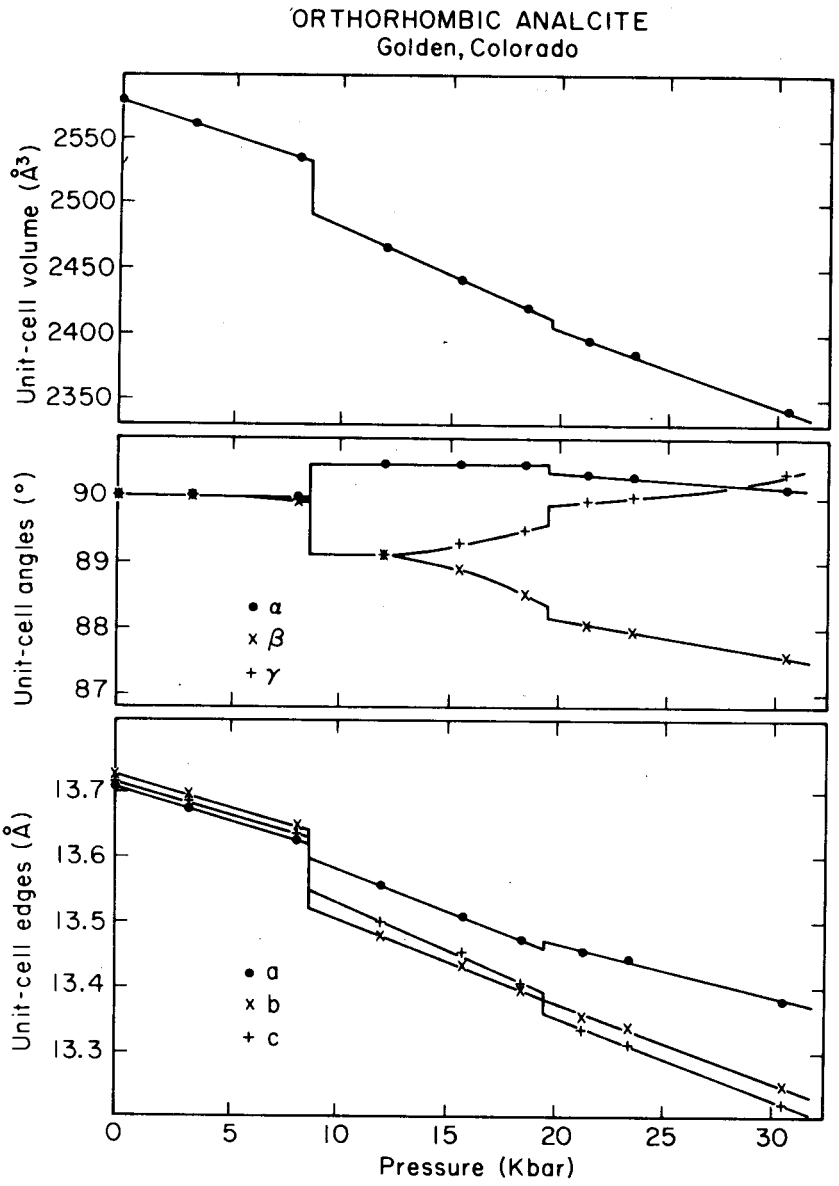

FIGURE 4 Unit-cell parameters vs. pressure for orthorhombic analcite from Golden, Colorado. Transformation behavior is similar to that illustrated in Figure 3, with volume changes at 8.5 and 19 kbar and dimensional symmetry changes at about 4 and 12 kbar.

TABLE V

Analcite unit-cell parameters, deviations from cubic dimensions, and suggested crystal systems at high pressure

P(kbar)	a(A)	b(A)	c(A)	α(°)	β(°)	γ(°)	V(A^3)	Δa^a(A)	$\Delta\alpha^a$(°)	System[a]
Cyclopian Islands Analcite—Tetragonal at room pressure										
0.001	13.708(2)[b]	13.709(2)	13.732(2)	89.98(2)	89.98(2)	89.97(2)	2580.5(6)	0.024(4)	0.03(2)	T+
1.5(5)	13.686(1)	13.694(2)	13.706(1)	89.99(1)	90.01(1)	89.99(1)	2568.8(4)	0.020(2)	0.01(1)	T+
3.5(5)	13.67(1)	13.67(1)	13.69(1)	89.95(5)	89.98(5)	90.01(5)	2555(10)	0.02(2)	0.05(5)	T+
5.0(5)	13.650(6)	13.649(6)	13.668(5)	89.96(3)	89.89(3)	89.93(4)	2545.3(1.7)	0.018(11)	0.11(3)	M′
6.0(5)	13.647(3)	13.643(4)	13.650(2)	89.97(2)	89.80(1)	89.86(2)	2541.5(9)	0.007(6)	0.20(1)	M′
7.0(5)	13.630(7)	13.565(9)	13.577(5)	90.41(4)	89.25(4)	89.24(4)	2510(2)	0.065(16)	0.76(4)	M′
9.0(5)	13.612(2)	13.539(3)	13.548(2)	90.42(2)	89.18(1)	89.23(2)	2496.1(8)	0.073(5)	0.82(1)	M′
12.5(1.0)	13.563(2)	13.506(3)	13.508(2)	90.52(2)	88.99(1)	89.13(2)	2473.6(8)	0.055(5)	1.01(1)	Tr
18.0(1.0)	13.497(7)	13.438(8)	13.439(4)	90.59(4)	88.70(4)	89.16(3)	2436(2)	0.059(15)	1.30(4)	Tr
19.0(1.0)	13.522(4)	13.394(3)	13.363(4)	90.34(2)	88.47(2)	90.05(3)	2422.0(1.2)	0.159(8)	1.53(2)	Tr
22.0(1.0)	13.480(4)	13.354(5)	13.322(4)	90.33(3)	88.01(2)	90.15(3)	2396.5(1.4)	0.158(8)	1.99(2)	Tr
23.0(1.0)	13.473(3)	13.347(2)	13.309(1)	90.27(1)	88.00(1)	90.16(2)	2391.8(7)	0.164(4)	2.00(1)	Tr
27.0(1.0)	13.403(3)	13.307(5)	13.261(3)	90.36(3)	87.60(3)	90.23(2)	2363.0(1.2)	0.142(6)	2.40(1)	Tr
Golden, Colorado, Analcite—Orthorhombic at room pressure										
0.001	13.703(2)	13.714(2)	13.724(3)	90.05(2)	90.01(1)	90.04(2)	2579.0(9)	0.021(5)	0.05(2)	O
3.2(5)	13.673(1)	13.685(1)	13.694(1)	89.97(1)	89.99(1)	90.00(1)	2562.3(4)	0.021(2)	0.03(1)	O
8.0(5)	13.625(1)	13.633(1)	13.644(1)	89.92(1)	89.88(1)	89.87(1)	2534.4(3)	0.019(2)	0.13(1)	M′
12.0(5)	13.554(20)	13.477(6)	13.502(10)	90.51(6)	89.1(1)	89.10(7)	2466(5)	0.077(26)	0.90(10)	M′
15.5(5)	13.507(12)	13.432(9)	13.462(14)	90.51(7)	88.91(7)	89.30(7)	2442(4)	0.075(21)	1.09(8)	Tr
18.5(5)	13.478(7)	13.397(7)	13.408(7)	90.51(5)	88.44(4)	89.49(5)	2419.9(2.2)	0.081(14)	1.56(4)	Tr
21.3(5)	13.457(5)	13.356(4)	13.333(6)	90.35(4)	88.04(3)	89.94(3)	2395.0(1.5)	0.124(11)	1.96(3)	Tr
23.4(5)	13.443(7)	13.340(4)	13.312(7)	90.30(4)	87.95(5)	90.06(4)	2385(2)	0.131(14)	2.05(5)	Tr
30.5(5)	13.381(6)	13.250(4)	13.222(6)	90.18(3)	87.59(4)	90.40(3)	2342.2(1.6)	0.159(12)	2.41(4)	Tr

[a] See Table IV for definitions.

[b] Parenthesized figures represent *esd*'s of least units cited.

confirm the existence of this phase transition from unit-cell data alone. If analcite at pressures below 12 kbar is pseudo-monoclinic, but triclinic in detail, then the 12-kbar "transition" is an artifact of the unit-cell data.

A fourth phase transition is indicated by the small (0.25 percent ΔV) volume change at 18.5 kbar for Cyclopian analcite and 20 kbar for Golden analcite. The transformation is characterized by another increase in deviations from cubic dimensions, with a triclinic reduced unit cell of $a = 11.4$, $b = 11.4$, $c = 11.7$ Å, $\alpha = 109.2$, $\beta = 110.0$, and $\gamma = 108.4°$ at 27 kbar for Cyclopian analcite. This triclinic phase has the largest deviation parameters, with $\Delta a > 0.12$ Å and $\Delta\alpha > 1.5°$. Distortion parameters increase with increasing pressure above the second volume discontinuity, but no further phase transitions were detected to 30 kbar.

All analcite high-pressure phase transitions appear to be rapid and reversible. By raising and lowering the pressure of the diamond cell while it was mounted on the diffractometer the position of the (008) reflection at both the 6.5 and the 18.5 kbar transitions of Cyclopian analcite was observed to change discontinuously. Single crystals of both Golden and Cyclopian analcite were preserved through several cycles of pressure up to 30 kbar.

In summary, both analcites, though of different crystal systems under room conditions, demonstrate similar dimensional variation with increasing pressure (Figures 3 and 4). Both specimens transform from orthogonal to *C*-centered monoclinic at about 4 kbar, have a volume discontinuity at about 8 kbar, transform from monoclinic to triclinic at about 12 kbar, and have a volume discontinuity at 19 kbar. Details of unit-cell changes from 0 to 30 kbar are also similar, with relative changes of the three unit-cell axes and three angles comparable for the two analcites.

A structural refinement of monoclinic or triclinic analcite at high pressure was not attempted because of twinning of the single crystal at high pressure. A triclinic analcite, furthermore, has more than 120 variable positional parameters in the asymmetric unit. To solve such a light-atom structure is probably beyond the present capabilities of diamond-cell procedures because of the limited access to reciprocal space afforded by the diamond cell (Merrill and Bassett, 1974b). A hemisphere of intensity data was collected on Cyclopian analcite at 27 kbar in order to search for violations of the original *I*-centering condition. No violations were observed, and the space group of triclinic analcite may be described as $I1$ or $I\bar{1}$ with the pseudo-cubic unit cell.

DISCUSSION

Although a complete structural analysis of the several high-pressure analcite phases is not possible at this time, the nature of the transitions may be described in terms of polyhedral tilting. All the observed structural properties

of analcite at high pressure are consistent with the criteria for polyhedral tilt transitions as defined above. Specifically:

1) The analcite structure is composed of rigid, corner-linked (Al, Si) tetrahedra, which enclose large cations and water sites.

2) The high-pressure phases are of lower symmetry or greater distortion from cubic dimensions than the low-pressure phases.

3) The transitions are rapid, reversible, and nonquenchable; single crystals are preserved through the transition.

4) Twinning was observed in the high-pressure phases.

5) The value of dP/dT is positive, 57 bar/°C, for the first transition (Rosenhauer and Mao, 1975), a value which is similar to those of 63 bar/°C for $\bar{\alpha}/\bar{\beta}$ for $^{VI}Na^+$ and 34 bar/°C for $^{VIII}Na^+$ predicted by Hazen and Prewitt (1977).

Analcite therefore conforms to all five criteria of polyhedral tilt transitions, and we hypothesize that these several high-pressure transitions are due to tilting of corner-linked Al-Si tetrahedra. The stable analcite modification, for a given composition and aluminum- and silicon-ordered distribution, is determined by the effective size of the large alkali site. With increasing pressure this site compresses more than the aluminum and silicon tetrahedra; the tetrahedral framework therefore must collapse or distort around the sodium sites. Transformations from orthogonal to monoclinic to triclinic forms facilitate collapse of the tetrahedral framework by decreasing the symmetry and thereby increasing the rotational or tilt degrees of freedom of individual tetrahedra. The two volume discontinuities presumably represent major increases in distortions of the alkali sites, with corresponding tilting of polyhedral elements but no change in polyhedral linkages.

CONCLUSIONS

Numerous common minerals and other compounds fulfill the structural criteria for polyhedral tilt transformations. All framework silicates have corner-linked arrays of rigid polyhedra; many of these materials are known to have high-temperature tilt transitions at room pressure and many should also have high-pressure transitions. Other silicates, including chain and ring structures, as well as borates and phosphates, may also have transitions involving reversible tilting of tetrahedral groups. Perovskite-type compounds have received considerable attention in recent years because of their electronic properties and because perovskites with silicon in octahedral coordination may be an important mineral phase in the earth's mantle. Perovskites are

well known to deviate significantly from the ideal cubic structure (note the cover illustration), and several polyhedral tilt transitions are known in synthetic perovskites (Megaw, 1974; Yagi *et al.*, 1978).

Polyhedral tilt transitions may cause significant changes in the distortions, and consequently the physical properties, of ionic compounds. Because these transitions are nonquenchable, it is not generally possible to recognize transformed material under room conditions. It is essential, therefore, to study materials that fulfill the structural criteria of polyhedral tilt transitions under conditions of interest rather than to extrapolate properties to high temperature or pressure.

Acknowledgments

The authors gratefully acknowledge Dr. Brian Mason of the Smithsonian Institution and Dr. Stewart Agrell of Cambridge University for providing the analcite specimens. Valuable reviews of this study were provided by Drs. H. K. Mao, D. Rumble III, and H. S. Yoder, Jr. The work was supported in part by NSF grant EAR77-23171.

References

Boccara, N. (1968) Second-order phase transitions characterized by a deformation of the unit cell. *Annals of Physics*, **47**, 40–64.

Buerger, M. J. (1951) Crystallographic aspects of phase transformations. In R. Smoluchowski, J. E. Mayer and W. A. Weyl, Eds., *Phase Transformations in Solids*, p. 183–209. John Wiley and Sons, Inc., New York. pp. 183–209.

Buerger, M. J. (1957) Reduced cells. *Z. Kristallogr.*, **109**, 42–60.

Buerger, M. J. (1972) Phase transformations. *Soviet Phys.—Crystallogr.*, **16**, 959–968.

Clarke, R. and L. Benguigui (1977) The tricritical point in $BaTiO_3$. *J. Phys. C—Solid State Phys.*, **10**, 1963–1973.

Cohen, L. H. and W. Klement, Jr. (1976) Effect of pressure on reversible solid-solid transitions in nepheline and carnegieite. *Mineral. Mag.*, **40**, 487–492.

Cohen, L. H., W. Klement, Jr., and H. G. Adams (1974) Yet more observations on the high-low quartz inversion: thermal analysis studies to 7 kbar with single crystals. *Am. Mineral.*, **59**, 1099–1104.

Coombs, D. S. (1955) X-ray investigation on wairakite and non-cubic analcime. *Mineral. Mag.*, **30**, 699–708.

Deer, W. A., R. A. Howie, and J. Zussman (1963) *Rock-Forming Minerals*, Vol. 4, *Framework Silicates*, pp. 338–350. John Wiley and Sons, Inc., New York.

Hamilton, W. C. (1974) Angle settings for four-circle diffractometers. In J. A. Ibers and W. C. Hamilton, Eds., *International Tables for X-Ray Crystallography*, Vol. IV, pp. 273–284. The Kynoch Press, Birmingham, England.

Hazen, R. M. (1976) Sanidine: predicted and observed monoclinic-to-triclinic reversible transformations at high pressure. *Science*, **194**, 105–197.

Hazen, R. M. (1977a) Mechanisms of transformation and twinning in gillespite at high pressure. *Am. Mineral.*, **62**, 528–533.

Hazen, R. M. (1977b) Temperature, pressure, and composition: structurally analogous variables. *Phys. Chem. Minerals*, **1**, 83–94.

Hazen, R. M. and L. W. Finger (1977) Modifications in high-pressure, single-crystal diamond-cell techniques, *Carnegie Inst. Wash. Year Book*, **76**, 655–656.

Hazen, R. M. and C. T. Prewitt (1977) Effects of temperature and pressure on interatomic distances in oxygen-based minerals. *Am. Mineral.*, **62**, 309–315.

Heur, A. H. and G. L. Nord, Jr. (1976) Polymorphic phase transitions in minerals. In H.-R. Wenk, Ed., *Electron Microscopy in Mineralogy*, pp. 274–303. Springer-Verlag, New York.

Langer, K. and W. Schreyer (1969) Infrared and powder X-ray diffraction studies of cordierite. *Am. Mineral.*, **54**, 1442–1459.

Larsen, E. S. and B. F. Buie (1938) Potash analcime and pseudoleucite from the Highwood Mountains of Montana. *Am. Mineral.*, **23**, 837–849.

Mazzi, F. and E. Galli (1978) Is each analcime different? *Am. Mineral.*, **63**, 448–460.

Megaw, H. D. (1973) *Crystal Structures: A Working Approach*. W. B. Saunders, Philadelphia.

Megaw, H. D. (1974) The seven phases of sodium niobate. *Ferroelectrics*, **7**, 87–89.

Merrill, L. and W. A. Bassett (1974a) The crystal structure of $CaCO_3$(II), a high-pressure metastable phase of calcium carbonate. *Acta Crystallogr.*, **B31**, 343–349.

Merrill, L. and W. A. Bassett (1974b) Miniature diamond anvil pressure cell for single crystal X-ray diffraction studies. *Rev. Sci. Instrum.*, **45**, 290–294.

Pauling, L. (1960) *The Nature of the Chemical Bond*. Cornell University Press, Ithaca, New York.

Piermarini, G. J., S. Block, J. D. Barnett, and R. A. Forman (1975) Calibration of the pressure dependence of the R_1 ruby fluorescence line to 195 kbar. *J. Appl. Phys.*, **46**, 2774–2780.

Rosenhauer, M. and H. K. Mao (1975) Studies on the high-pressure polymorphism of analcite by powder X-ray diffraction and differential thermal analysis methods. *Carnegie Inst. Wash. Year Book*, **74**, 413–415.

Smyth, J. R. (1974) Experimental study on the polymorphism of enstatite. *Am. Mineral.*, **59**, 345–352.

Strens, R. G. J. (1967) Symmetry-entropy-volume relationships in polymorphism. *Mineral. Mag.*, **36**, 565–577.

Wilkinson, J. F. G. (1968) Analcimes from some potassic igneous rocks and aspects of analcime-rich igneous assemblages. *Contrib. Mineral. Petrol.*, **18**, 252–269.

Yagi, T., H. K. Mao and P. M. Bell (1978) Structure and crystal chemistry of perovskite-type $MgSiO_3$. *Phys. Chem. Minerals*, **3**, 97–110.

Yoder, H. S., Jr. and C. E. Weir (1960) High-pressure form of analcite and free energy change with pressure of analcite reactions. *Am. J. Sci.*, **258A**, 420–433.